Late Cretaceous Polar Wander of the Pacific Plate: Evidence of a Rapid True Polar Wander Event

William W. Sager[1]* and Anthony A. P. Koppers[2]

We reexamined the Late Cretaceous–early Tertiary apparent polar wander path for the Pacific plate using 27 paleomagnetic poles from seamounts dated by $^{40}Ar/^{39}Ar$ geochronology. The path shows little motion from 120 to 90 million years ago (Ma), northward motion from 79 to 39 Ma, and two groups of poles separated by 16 to 21 degrees with indistinguishable mean ages of 84 ± 2 Ma. The latter phenomenon may represent a rapid polar wander episode (3 to 10 degrees per million years) whose timing is not adequately resolved with existing data. Similar features in other polar wander paths imply that the event was a rapid shift of the spin axis relative to the mantle (true polar wander), which may have been related to global changes in plate motion, large igneous province eruptions, and a shift in magnetic field polarity state.

An apparent polar wander path (APWP) shows past locations of Earth's spin axis, defined as the time-averaged paleomagnetic pole, relative to a given lithospheric plate. Although it is widely accepted that plate motion is the main cause of APW, drift of the spin axis relative to the mantle (termed "true polar wander" or TPW) is also a contributor. This phenomenon may be the result of changes in Earth's maximum principal axis of inertia caused by redistribution of mass in the mantle (*1*). TPW has accounted for 15° to 20° of polar motion in the past 200 million years (My) [for example, (*2–4*)], but short-lived TPW events may have occurred with rates exceeding plate velocities, leading to large shifts in paleogeographic zones (*5*).

Numerous hot spots and rapid tectonic motions have left an unparalleled, 140-My record of plate motion relative to the mantle on the Pacific plate (*6, 7*). Consequently, Pacific paleomagnetic data are important because they allow TPW to be measured using differences between the paleomagnetic and hot spot (mantle) reference frames [see review in (*8*)]. Pacific paleomagnetic data are atypical because it is difficult to acquire oriented samples, given that the ocean covers virtually the entire plate. Ocean drilling cores and studies of young islands provide some data but are insufficient to delineate Pacific APW in detail. In consequence, magnetic modeling has been used to calculate Pacific paleomagnetic poles, mainly by seamount magnetic anomaly inversion and determination of sea-floor magnetic lineation asymmetry (skewness). Currently, the Pacific APWP is defined by 8 to 10 mean poles ranging in age from Early Cretaceous to middle Tertiary (Fig. 1A) (*9–11*).

We report a revised Late Cretaceous– early Tertiary APWP determined from 27 Pacific seamounts dated by $^{40}Ar/^{39}Ar$ geochronology. This analysis was done because of the availability of new and revised seamount data and discrepancies between the accepted Pacific APWP and new data from other sources. For simplicity, the analysis was limited to seamount paleopoles because these are the predominant data for the time period.

[1]Department of Oceanography, Texas A&M University, College Station, TX 77843, USA. [2]Institute of Geophysics and Planetary Physics, Scripps Institution of Oceanography, University of California, San Diego, La Jolla, CA 92093, USA.

*To whom correspondence should be addressed. E-mail: wsager@ocean.tamu.edu

A

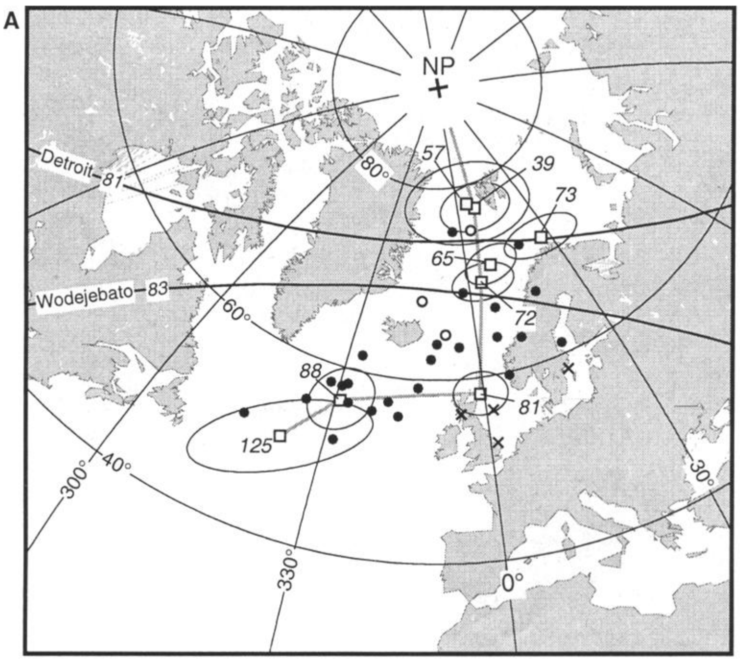

B

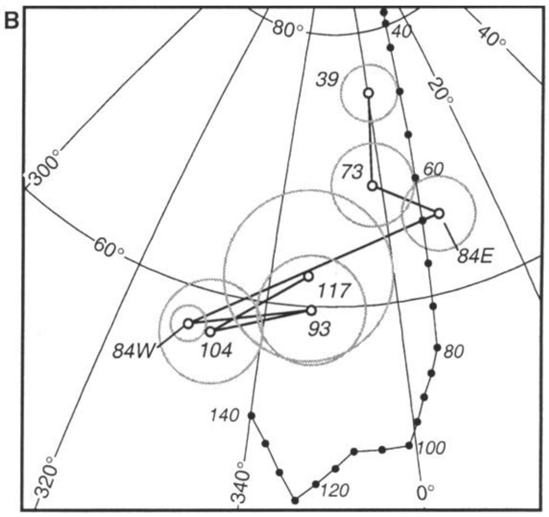

Fig. 1. **(A)** Paleomagnetic poles and the Pacific APWP. Small filled circles denote seamount paleomagnetic poles with normal polarity; open circles, reversed polarity. Crosses denote poles from undated, reversed-polarity seamounts, possibly formed during Chron 33r (*21*). Open squares connected by heavy gray lines show mean paleomagnetic poles defining the APWP (*9–11*). Ages (Ma) are given in italics, and surrounding ellipses are 95% confidence regions. Arcs labeled "Detroit" (*18*) and "Wodejebato" (*19*) are paleo-colatitudes from Chron 33r–age ODP cores. **(B)** Pacific polar wander path (heavy line) derived from seamount paleomagnetic poles. Ages and confidence regions are shown as in (A); the eastern and western 84-Ma poles are denoted 84E and 84W. Filled circles show the predicted polar wander path, with points at 5-My intervals, derived from a plate versus hot spot motion model (*7*). TPW is the favored explanation of much of the difference between observed and predicted APWPs.

Paleomagnetic pole analysis. The shape and magnetic anomaly of a seamount can be measured from a surface ship and used to calculate a seamount's mean magnetization vector, which can in turn be used to calculate a paleomagnetic pole (*12*). Our reliability criteria were slightly more stringent than those of previous analyses because paleopoles from well-dated seamounts are more plentiful (*13*). In addition, we considered only seamounts with $^{40}Ar/^{39}Ar$ radiometric dates because this method produces the most reliable dates for altered submarine basalts (*14*).

Twenty-seven seamount paleomagnetic poles (Table 1) were grouped by age and similar pole location into seven groups: 39 million years ago (Ma), 66 to 79 Ma, 82 to 86 Ma (two groups), 91 to 97 Ma, 102 to 108 Ma, and 113 to 120 Ma. Mean pole positions were calculated using standard Fisher statistics with equal weighting for each pole (*15*). A mean age and standard deviation (Table 2) were calculated for each group using simple arithmetic averages (*16*).

Pacific apparent polar wander path. Our APWP has similarities and differences relative to prior versions. Similar to published Pacific APWPs (*9–11*), the latest Cretaceous and early Tertiary poles are near the 0° meridian and trend northward, whereas older poles cluster near 60°N, 340°E (Fig. 1B) and have overlapping confidence circles that imply slow polar movement. A major difference is that there is no pole in the location of the previous 81-Ma pole (Fig. 1A). Instead, the 82- to 86-Ma data produce two poles located 20.5° ± 2.5° (1σ) apart. Previously, this discrepancy was attributed to microplate rotations in the Musicians and South Hawaiian seamounts (*17*). We think that this interpretation is incorrect and that the two poles differ in age, with the western pole slightly older, and that there was a rapid shift in pole position. Because the two 84-Ma poles are the farthest apart of Cretaceous poles, a more conservative estimate of the polar shift is 16.3° ± 2.7°, based on the distance between the eastern 84-Ma pole and the average of older poles [58.9°N, 337.4°E; A_{95} (the radius of the 95% confidence cone) = 3.5°]. The new APWP eliminates the discrepancy of the prior 81-Ma pole versus recent Ocean Drilling Program (ODP) basalt core data from Detroit Guyot at 81 Ma (*18*) and Wodejebato Guyot at 83 Ma (*19*) or a pole from Chron 33r (79 to 83 Ma) skewness (*20*)—all of which are consistent with the younger (eastern) 84-Ma pole (Fig. 1A).

Although the two 84-Ma poles have indistinguishable ages, we think that the polar shift occurred just before Chron 33r, because all the 82- to 86-Ma seamounts have normal polarities and data from that reversed-polarity period are consistent with latest Cretaceous poles. Despite normal polarities, three of the 82- to 86-Ma seamounts have ages within Chron 33r. These seamounts probably have dates that slightly underestimate their true ages. It is also possible that the two 84-Ma poles bracket the shift because poles from three reversely polarized seamounts, thought to have formed during Chron 33r (*9, 10, 21*), are midway between the two 84-Ma poles. These three poles were not included in our analysis because the seamounts are not radiometrically dated.

Is the polar shift an artifact? Although seamount poles are probably not as reliable as standard paleomagnetic data, the 84-Ma polar shift is not readily explained by seamount

Table 1. Paleomagnetic (Paleomag.) and age data. For seamounts with poles calculated by least squares inversion (*12*), the GFR is the ratio of the sum of field values divided by the sum of residuals. For seamounts with poles calculated by seminorm inversion (*12*), the 95% confidence (conf.) ellipse dimensions Maj and Min are the major and minor semiaxis lengths; Az is the azimuth from north of the major semiaxis.

Seamount name	Location		Paleopole		GFR	95% conf. ellipse			Age (Ma) ± S1σ	Reference	
	°N	°E	°N	°E		Maj	Min	Az		Paleomag.	Age
					Radiometric dates						
Abbott	31.8	174.3	75.5	4.6*	6.6				38.7 ± 0.9	(*45*)	(*55*)
Stanley	8.2	198.1	75.6	356.5	4.7				39.3 ± 1.5	(*46*)	(*56*)
Paumakua	24.9	202.9	64.8	352.1*		6.8	1.8	63	65.5 ± 4.3	(*47*)	(*17*)
Wageman	−7.5	208.5	68.5	345.6*	3.1				71.9 ± 1.4	(*46*)	(*56*)
Haydn	26.6	198.7	69.2	357.9	3.3				75.1 ± 1.2	(*17*)	(*43*)
Mendelssohn-E	25.1	198.3	67.3	18.1		9.7	3.3	78	78.5 ± 0.9	(*47*)	(*43*)
Mendelssohn-W	25.1	197.2	63.5	355.6		12.9	4.2	65	82.4 ± 1.3	(*47*)	(*43*)
Khatchaturian	28.1	197.7	56.5	332.5	5.3				82.5 ± 2.5	(*48*)	(*43*)
Kapsitotwa	12.1	194.2	58.1	330.5		10.1	4.0	47	82.7 ± 3.6	(*49*)	(*57*)
Schumann-W	25.7	199.8	63.3	10.7		13.8	4.1	78	83.0 ± 1.0	(*47*)	(*43*)
Nagata	12.5	193.0	67.1	6.3		9.2	4.4	62	85.0 ± 1.1	(*49*)	(*56*)
Liszt	29.0	197.7	58.5	331.6		6.6	2.2	50	84.4 ± 1.5	(*47*)	(*43*)
Cross	18.5	202.0	72.4	19.4	4.2				84.6 ± 3.8	(*17*)	(*17*)
Rachmaninov	29.6	196.7	55.6	324.6	2.5				86.4 ± 1.2	(*48*)	(*43*)
H11	26.5	182.2	61.3	18.9		9.2	2.9	104	86.4 ± 0.6	(*49*)	(*58*)
Wilde	21.2	163.3	61.8	333.1		7.1	2.1	82	90.6 ± 0.3	(*50*)	(*59*)
Mahler	31.8	195.0	56.0	342.6	6.7				91.0 ± 0.7	(*17*)	(*43*)
Makarov	29.5	153.6	59.2	346.2		2.9	0.9	103	93.9 ± 1.3	(*50*)	(*59*)
Miami	21.7	161.9	59.8	5.9		6.5	2.1	116	96.8 ± 0.6	(*49*)	(*59*)
Scripps	23.7	159.3	63.9	350.2		11.1	2.1	87	101.6 ± 0.7	(*50*)	(*59*)
Golden Dragon	21.3	153.2	56.2	337.4		5.6	1.9	98	102.1 ± 0.2	(*50*)	(*7*)
Isakov	31.6	151.2	52.3	331.5		4.2	1.7	87	103.7 ± 1.8	(*50*)	(*59*)
Mij-Lep (Heezen)	8.8	163.2	57.4	340.3	3.4				106.0 ± 1.0	(*51*)	(*7*)
Winterer	32.8	148.4	51.6	315.5		4.1	1.5	97	108.3 ± 1.0	(*50*)	(*59*)
Lo-En	10.1	162.8	64.0	5.0	3.0				113.1 ± 0.5	(*52*)	(*60*)
Takuyo-Daisan	34.2	144.3	58.2	328.2		4.3	1.9	96	118.1 ± 1.1	(*50*)	(*7*)
Daiichi-kashima	35.8	142.7	62.3	348.8	3.1				120.2 ± 2.6	(*53*)	(*61*)
					Polarity dates						
C6	14.9	187.7	55.0	1.8*	2.0				83	(*10*)	(*10*)
Kona 5S	17.1	205.8	49.8	1.5*	2.9				79–83	(*54*)	(*9*)
Show	17.9	207.3	57.1	355.3*		6.2	2.7	63	79–83	(*47*)	(*9*)
Chatauqua	22.2	197.4	57.3	18.2*		9.7	3.6	95	79	(*47*)	(*9*)

*Reversed polarity.

modeling errors. One possible error is the result of induced or viscous magnetization in the present field direction, combined with the remanent magnetization that was acquired during volcanic emplacement (*22*). Measured induced magnetizations from seamount rock samples are 10 to 25% (*23*), implying changes of 2° to 6° in the pole location for Pacific seamounts. Although a few seamounts have poles that imply larger bias, most mean seamount poles closely agree with other paleomagnetic data (*10*). More important, the shift is nearly perpendicular to the direction in which induced and viscous magnetization would bias the poles (*24*).

Another problem is inaccuracy caused by violation of the modeling assumption of uniform magnetization (*25*). There should be no consistency among heterogeneities in different seamounts, so their effect should be random pole scatter. The mean standard error of dated seamount poles relative to the mean pole positions is only 5.6° (*26*), and because the two 84-Ma poles are statistically different at the 99.9% level (*27*), it is unlikely that these two groups are a result of random errors.

Late Cretaceous shifts in other apparent polar wander paths. Similar Late Cretaceous polar shifts are observed in other APWPs. To compare the direction of polar movement in different APWPs, we removed the effects of plate motions by examining the APWPs in their hot spot reference frames (*28*). The Pacific plate displays rapid polar shift toward ~160° longitude (Fig. 2). The North American plate shows a similar shift of 13° that coincides with Chron 33r (*29*) (Fig. 2). Synthetic global average APWPs (*3, 4*) also display rapid polar movement in a direction close to that of the Pacific APWP, although the timing is not precisely the same, probably because these composite APWPs were smoothed with 20- and 30-My moving windows. APWP similarities in different parts of the globe imply that the Pacific polar shift is a real and global phenomenon with a consistent direction in the mantle reference frame.

Table 2. The seven groups of mean paleomagnetic poles and their ages. A_{95} is the radius of the 95% confidence cone; k is Fisher's concentration parameter.

ID	N	Location °N	Location °E	A_{95}	k	Age (Ma) ± SD
39	2	75.6	0.6	4.4	3210	39.0 ± 0.4
73	4	67.9	358.4	6.4	204	72.8 ± 5.5
84E	5	65.8	9.8	5.7	183	84.3 ± 1.6
84W	4	57.2	329.7	2.7	1155	84.0 ± 1.8
93	4	59.7	347.0	8.3	123	93.1 ± 2.9
104	5	56.8	333.8	8.1	89	104.3 ± 2.8
117	3	62.3	346.2	14.2	77	117.1 ± 3.6

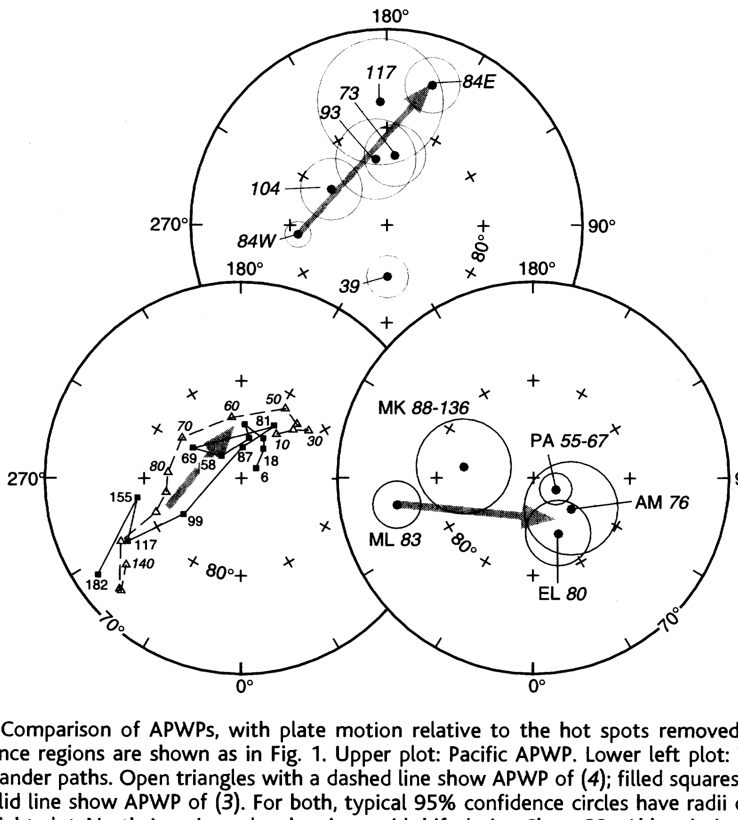

Fig. 2. Comparison of APWPs, with plate motion relative to the hot spots removed. Ages and confidence regions are shown as in Fig. 1. Upper plot: Pacific APWP. Lower left plot: Two global polar wander paths. Open triangles with a dashed line show APWP of (*4*); filled squares connected by a solid line show APWP of (*3*). For both, typical 95% confidence circles have radii of 4° to 6°. Lower right plot: North America poles showing rapid shift during Chron 33r. Abbreviations [see (*29*), and references therein]: AM, Adel Mountain; EL, Elkhorn Mountains; MK, mid-Cretaceous reference pole; ML, Maudlow Formation; PA, Paleocene reference pole. Shaded gray arrows show the sense of the polar shift in each plot.

What caused the polar shift? A shift in paleomagnetic poles can be caused by three phenomena: (i) plate motion; (ii) rapidly changing long-term, nondipole, geomagnetic field components; and (iii) TPW. Of these, TPW is most consistent with the observations. TPW should have a consistent direction measured from all parts of the globe, so similarities in timing and direction of the APWP shifts (Fig. 2) are a strong argument for TPW. Plate motion is an unlikely explanation because the rotation required to account for the polar motion would have caused highly curved seamount chains on the Pacific plate or seamount chains that become younger westward, neither of which are observed (Fig. 3) (*30*). Microplate rotation is also unlikely because seamounts from the two 84-Ma groups cannot be neatly divided into geographically distinct regions that can be ascribed to simple block rotations.

Nondipole field changes are also an unlikely explanation because the polar shift is inconsistent with studies of the time-averaged geomagnetic field, which show only small (<5 to 10% of the dipole), axial, nondipole components (*3*). The pole shift results in a declination change in the central Pacific and would require unexpectedly large nonaxial field components (for example, an equatorial dipole 36% of the strength of the axial dipole).

Implications. The Pacific APWP indicates a 16° to 21° pole shift in ~2 to 5 My. At 3° to 10° per My, this polar motion is far faster than the most rapid plate motions occurring today relative to the mantle (~0.8° per My) and similar to that proposed for a large TPW event at the beginning of the Cambrian (*5*). Because of the rapidity of the 84-Ma shift, it is not well resolved in most APWPs owing to sparse data. Hence, other similar events may also be unrecognized.

The 84-Ma TPW episode coincides with numerous tectonic events. At about the same time, plate reorganizations began in all ocean basins (*31–33*). From 85 to 90 Ma, several large igneous provinces [Kerguelen Plateau (*34*), Ontong Java Plateau (*35*), and the Carib-bean-Columbian Cretaceous Igneous Province

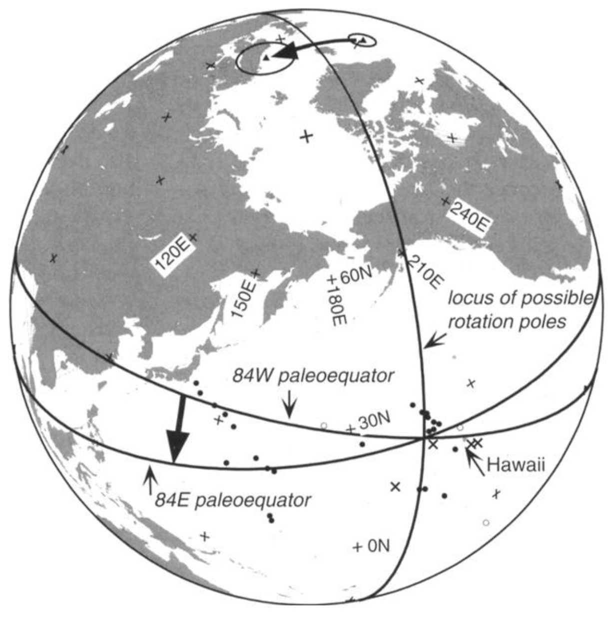

Fig. 3. Locations of seamounts used in this study and paleoequator change implied by shift in 84-Ma poles. Filled (normal polarity) and open (reversed polarity) circles show the locations of seamounts used in calculations; crosses show possible Chron 33r–age seamounts dated by magnetic polarity (*21*). Two transverse circular arcs show paleoequator locations inferred from the two 84-Ma poles. Arrows show the sense of rotation (old to young). The longitudinal circle is the locus of points that describe potential rotation poles that would bring the two paleomagnetic poles (triangles) into coincidence.

(*36*)] were erupting. Additionally, the geomagnetic field began reversing polarity at 83 Ma after a long period of constant polarity. A possible link is a mantle overturn event (*37*) that redistributed mass anomalies in the mantle (causing TPW), initiated large mantle plume eruptions, changed reversal frequency by modifying heat flux across the core-mantle boundary, and caused a global plate reorganization.

Another implication of the TPW event is rapid latitude changes in various locales. Those effects would be most pronounced 90° from the TPW rotation axis, where the latitude shift would equal the 16° to 21° rotation. The Atlantic-bordering continents were in just that position. We calculate that the sites of Washington, D.C., and Dakar, Senegal, would have shifted south 15° to 20° (*38*). This raises the question of how these sites returned to their present latitudes. A different episode of TPW apparently occurred between 81 and 43 Ma, and it moved the globe approximately the same amount in nearly the opposite direction (*11, 18, 39, 40*). Together, these events suggest a broader TPW episode that spanned most of the Late Cretaceous.

References and Notes

1. P. Goldreich and A. Toomre, *J. Geophys. Res.* **74**, 1555 (1969).
2. C. G. A. Harrison and T. Lindh, *Nature* **300**, 251 (1982).
3. R. A. Livermore, F. J. Vine, A. G. Smith, *Geophys. J. R. Astron. Soc.* **79**, 939 (1984).
4. J. Besse and V. Courtillot, *J. Geophys. Res.* **96**, 4029 (1991).
5. J. L. Kirschvink, R. L. Ripperdan, D. A. Evans, *Science* **277**, 541 (1997).
6. P. Wessel and L. W. Kroenke, *Nature* **387**, 365 (1997).
7. A. A. P. Koppers, thesis, Free University, Amsterdam (1998).
8. R. G. Gordon, *Annu. Rev. Earth Planet. Sci.* **15**, 567 (1987).
9. ———, *Geophys. Res. Lett.* **10**, 709 (1983).
10. W. Sager and M. S. Pringle, *J. Geophys. Res.* **93**, 11753 (1988).
11. K. E. Petronotis and R. G. Gordon, *Geophys. J. Int.* **139**, 227 (1999).
12. Pacific seamount paleopoles have been derived using two similar inversion methods that produce comparable pole estimates. Both solve for a magnetization that approximates the magnetic anomaly shape and amplitude given the measured seamount topography. The least squares method assumes a uniform magnetization and simply minimizes residuals between observed and calculated anomalies [for example, M. L. Richards, V. Vacquier, G. D. Van Voorhis, *Geophysics* **32**, 678 (1967)]. The seminorm method calculates a maximally uniform solution consistent with a magnetization containing random inhomogeneities [R. L. Parker, L. Shure, J. A. Hildebrand, *Rev. Geophys.* **25**, 17 (1987)]. The least squares method makes no error estimate, but a 95% confidence ellipse for the paleopole can be calculated with the seminorm method (*41*). However, our calculations indicate that these error bounds may underestimate the true error [see (*15*)].
13. Most prior analyses used the goodness-of-fit ratio (GFR), the mean of observed anomaly values divided by the mean of residuals (observed minus calculated anomalies), as a reliability criterion, rejecting results with GFR < 2.0. The GFR is an inadequate criterion for seminorm models because this method matches the observed anomaly to arbitrarily high precision owing to its inclusion of inhomogeneities in the magnetization model. Consequently, there is no accepted reliability criterion for such data. We rejected data with GFR < 2.5 and 95% confidence ellipse major semiaxes $> 14°$. Both criteria are arbitrary, but their effect is to remove from consideration seamounts with complex magnetic anomalies that are poorly modeled by these methods and therefore may violate model assumptions.
14. Seawater alteration can add potassium to seamount basalts, resulting in ages that are too low when using the conventional K-Ar technique [R. J. Fleck, J. F. Sutter, D. H. Elliot, *Geochim. Cosmochim. Acta* **41**, 15 (1977)]. Using $^{40}Ar/^{39}Ar$ incremental heating techniques, the imprint of alteration can be monitored and high-quality ages can be calculated on the basis of undisturbed sections within age spectra (*42, 43*) [A. A. P. Koppers, H. Staudigel, J. R. Wijbrans, *Chem. Geol.*, in press].
15. We used simple Fisher statistics to calculate mean paleomagnetic poles and 95% confidence circles. The poles were divided into groups on the basis of clustering of dates and pole positions (Web fig. 1 at *Science* Online, www.sciencemag.org/feature/data/1042962.shl). We tried using a moving window in time, as is done in some APWP calculations, but most windows were empty when small window widths were used. Only the 82- to 86-Ma group had to be separated by pole position because it was obvious that the poles of that age group contained far more scatter than any other. More elaborate schemes for pole and error calculations were rejected because seamount paleomagnetic pole errors are poorly quantified. Because some seamount poles may be more accurate than others, it may be desirable to weight poles by their error estimates [for example, R. G. Gordon and A. Cox, *Geophys. J. R. Astron. Soc.* **63**, 619 (1980)]. However, confidence limits are not routinely calculated with the least squares inversion technique. Additionally, although a routine for calculating errors in seminorm inversion data has been developed (*41*), its reliability has been questioned (*25*). Our calculations using seminorm poles and confidence regions with the error-propagation method of Gordon and Cox indicate that estimated seminorm method–derived confidence ellipses are inconsistent with observed misfits between individual and mean paleomagnetic poles. Moreover, the implication is that the error estimates are too small. We tried to find a relation between pole misfit and GFR or the size of the seminorm 95% confidence ellipse major semiaxis, but the correlation was poor. Given the unknowns in pole uncertainties and the small amount of data used to calculate each mean pole (Table 2), the Fisher approximation seems adequate.
16. Mean pole ages can be calculated from multiple seamount ages using averages inversely weighted by analytical errors. However, this produces unrealistically small estimates of the standard deviation. This behavior reflects the fact that analytical errors for individual basalt ages are significantly smaller than the age range for typical seamount shield-building volcanism, which may last for as long as 5 to 10 My (*42*) [A. Abdel-Monem and P. W. Gast, *Earth Planet. Sci. Lett.* **2**, 415 (1967); D. A. Clague *et al.*, in *The Geology of North America, Vol. N, The Eastern Pacific and Hawaii*, E. L. Winterer, D. M. Hussong, R. W. Decker, Eds. (Geological Society of America, Boulder, CO, 1989), pp. 187–287; M. S. Pringle, H. Staudigel, J. Gee, *Geology* **19**, 363 (1991)]. The processes causing such prolonged seamount volcanism are still poorly understood, but they seem to be a function of tectonic setting [D. Epp, *J. Geophys. Res.* **89**, 11273 (1984); J. P. Morgan, W. J. Morgan, E. Price, *J. Geophys. Res.* **100**, 8045 (1995); P. Wessel, *Science* **277**, 802 (1997)]. For these reasons, calculating weighted averages based on analytical errors may significantly underestimate the actual geological error on average seamount ages and, by inference, on the mean magnetic pole ages.
17. W. Sager and M. S. Pringle, in *Seamounts, Islands, and Atolls*, B. Keating, P. Fryer, R. Batiza, G. Boehlert, Eds. (American Geophysical Union, Washington, DC, 1987), pp. 133–162.
18. J. A. Tarduno and R. D. Cottrell, *Earth Planet. Sci. Lett.* **153**, 171 (1998).
19. J. A. Tarduno and J. Gee, *Nature* **378**, 477 (1995).
20. S. M. Vasas, K. E. Petronotis, R. G. Gordon, *EOS Trans. Am. Geophys. Union* **75**, 203 (1994).
21. Four seamount poles come from seamounts that have reversed magnetic polarity that has been used to infer formation during Chron 33r. The initial argument was applied to three seamounts (Kona 5S, Show, Chatauqua) by Gordon (*9*). His logic was that the seamounts are reversed in polarity and have paleomagnetic poles well to the south of latest Cretaceous poles. Because Chron 33r at 79 to 83 Ma [S. C. Cande and D. V. Kent, *J. Geophys. Res.* **97**, 13917 (1992)] was the only long reversed-polarity period before the latest Cretaceous (the next significant reversed period is Chron 31r at 70 to 72 Ma), these seamounts may have formed during Chron 33r. Sager and Pringle (*10*) added seamount C6 and noted that this seamount was normal with a reversed-polarity top, so it probably formed at the beginning of Chron 33r; they also noted that Chatauqua is reversed-polarity with a normal top, so it may have formed at the end of Chron 33r. Although these

inferences were helpful at a time when few reliable radiometric dates were available, we decided it was inappropriate to insert these data into an otherwise well-dated data set. They are mentioned here because the location of three of these seamount poles is in the gap between older and younger Cretaceous poles and suggests, albeit weakly, that the polar shift occurred coincident with Chron 33r.

22. J. Gee, H. Staudigel, L. Tauxe, T. Pick, Y. Gallet, *J. Geophys. Res.* **98**, 11743 (1993).
23. J. Gee and M. Nakanishi, *Proc. Ocean Drill. Program Sci. Results* **144**, 615 (1995).
24. The magnetization calculated using seamount anomaly inversion is a combination of the original magnetization acquired during cooling of the seamount basalts along with any secondary magnetization superimposed by other geologic factors. Of particular importance are induced magnetization, caused by the present-day geomagnetic field, and viscous magnetization, resulting from reorientation of the magnetization with time. Both of these are usually removed from standard paleomagnetic samples by alternating field or thermal demagnetization and measurement in a field-free space. Although many seamount basalts have stable magnetic directions and remanent magnetizations that are much larger than their induced counterparts, one might expect both induced and viscous magnetization bias to affect seamount paleomagnetic poles (*22, 23*). We cannot completely investigate this effect with seamount samples because dredged and drilled rocks typically represent only a small fraction of the seamount exterior, and for most seamounts even these samples do not exist. Studies of seamount rocks (*22, 23*) indicate that the induced magnetization represents 10 to 25% of the total magnetization. Because we know that most Pacific seamounts formed 20° to 30° south of their present positions, we can calculate that this degree of bias would cause a 2° to 6° shift in pole position for normally magnetized seamounts. This shift is small because of the small angle between the present-day and paleofield directions. The shift can be larger for reversely polarized seamounts because the induced and viscous magnetizations are in the opposite direction from the original magnetization. We know in what direction induced and viscous bias will move a seamount pole. With this bias, the pole of a normally polarized seamount will move from the zero-bias position toward the geomagnetic pole (in northern Greenland). The pole of a reversely magnetized seamount will move in the opposite direction until the bias is much greater than the original magnetization. Our argument that the polar shift is not caused by induced or viscous bias is based on the fact that the shift is nearly perpendicular to the direction of pole shift expected from this bias.
25. R. L. Parker, *J. Geophys. Res.* **96**, 16101 (1990).
26. To obtain an estimate of the amount of pole scatter that is representative of our data set, we calculated the distance and angle of each seamount pole from the location of the mean paleomagnetic pole for that seamount's age group. Given the uncertainties in seamount anomaly inversion results, the scatter is small, with a ψ_{63} angle of 5.6° (this is the radius of the cone within which 63% of poles fall relative to the mean). The scatter in an east-west direction seems somewhat larger than that in the north-south direction (Web fig. 2 at *Science* Online, www.sciencemag.org/feature/data/1042962.shl) because a given error in inclination produces only about half the error in pole space, as does an equivalent error in declination. A better calculation of mean pole locations and errors would take this anisotropy into account; however, all the mean poles were determined with small numbers of poles with uncertainties that are poorly quantified, so more sophisticated analysis may not be entirely appropriate and would not change the results significantly.
27. P. L. McFadden and F. J. Lowes, *Geophys. J. R. Astron. Soc.* **67**, 19 (1981).
28. To compare the directions of APWP segments and to identify similarities, we needed to remove the effects of plate motions. One way to do this is to remove motions relative to the hot spots. Although there is still considerable debate about the fixity of hot spots in the mantle and whether they constitute a reliable and accurate reference frame, many authors have used and continue to use motions of plates relative to the hot spots for tectonic studies. Of all the plates, the motion of the Pacific plate relative to the hot spots is probably the best known (*6, 7*), particularly for the period represented by the Hawaiian-Emperor chain (81 Ma to present). There is a discrepancy when trying to compare results from Pacific hot spots and those in the Indian and Atlantic oceans [G. D. Acton and R. G. Gordon, *Science* **263**, 1246 (1994)], so we reconstructed Pacific data to the Pacific hot spots and other APWPs using Atlantic and Indian hot spots, with the assumption that the Pacific hot spots are fixed relative to those elsewhere. Pacific data were backtracked using the model of Koppers (*7*). Because this model has taken into account numerous Cretaceous seamount dates and several western Pacific seamount chains, it represents a significant improvement on prior models of Early Cretaceous Pacific plate motion. The two global synthetic APWPs (*3, 4*) were backtracked by their authors relative to the Atlantic and Indian hot spots. Although the details of the reconstructions were somewhat different, both are based on Morgan's models [W. J. Morgan, *Tectonophysics* **94**, 123 (1983)] and so the results are comparable. Given that our comparison was only for major trends, we did not redo these reconstructions. For the North America data, we backtracked using a more recent plate–hot spot model (*44*). The difference caused by using this updated plate motion model should be small.
29. J. F. Diehl, *J. Geophys. Res.* **96**, 9887 (1991).
30. Figure 3 shows the sense of motion needed to explain the pole shift at 84 Ma. In the central Pacific, this appears as a counterclockwise rotation. A microplate rotation (*17*) was a possible explanation as long as the poles that did not seem to fit the APWPs (i.e., those of the 84E group) were all in the Musicians and South Hawaiian seamounts (the latter group is near the present-day Hawaiian Islands but not formed by the Hawaiian hot spot). However, even this initial explanation was based on the presumption of two separate microplates rotating the same amount (a fortuitous occurrence). The 84E group contains two seamounts (H11 and Nagata) that are located more than 1500 km from the purported microplates. Thus, the circumstances that would cause all of these seamounts to rotate the same amount are even more unlikely. Could the shift be attributed to a rapid rotation of the Pacific plate as a whole? This seems unlikely for two reasons. First, by Late Cretaceous time, the Pacific plate was large and had slabs engaged along most of its northern and western margins [T. W. C. Hilde, S. Uyeda, L. Kroenke, *Tectonophysics* **39**, 145 (1977)]. A large rotation would have required those subduction zones to adopt strike-slip motions and drag slabs laterally through the mantle—an implausible explanation. Second, this rotation would have created highly arcuate seamount chains or chains with a younging-westward trend (as opposed to the observed younging-eastward trends), but no chains have been observed to fit this description. Consequently, there is no evidence suggesting a large rotation of the Pacific plate in its entirety.
31. T. Atwater, in *The Geology of North America, Vol. N, The Eastern Pacific and Hawaii*, E. L. Winterer, D. M. Hussong, R. W. Decker, Eds. (Geological Society of America, Boulder, CO, 1989), pp. 21–72.
32. K. D. Klitgord and H. Schouten, in *The Geology of North America, Vol. M, the Western North Atlantic Region*, P. R. Vogt and R. E. Tucholke, Eds. (Geological Society of America, Boulder, CO, 1986), pp. 351–378.
33. J.-Y. Royer, P. Patriat, H. W. Bergh, C. R. Scotese, *Tectonophysics* **155**, 235 (1988).
34. M. S. Pringle, *EOS Trans. Am. Geophys. Union* **78** (fall suppl.), F728 (1997).
35. M. L. G. Tejada, J. J. Mahoney, R. A. Duncan, M. P. Hawkins, *J. Petrol.* **37**, 361 (1996).
36. A. C. Kerr, J. Tarney, G. F. Mariner, A. Nivia, A. D. Saunders, *in Large Igneous Provinces: Continental, Oceanic, and Planetary Flood Volcanism*, J. J. Mahoney and M. F. Coffin, Eds. (American Geophysical Union, Washington, DC, 1997), pp. 123–144.
37. M. Stein and A. W. Hoffman, *Nature* **372**, 63 (1994).
38. Figure 3 indicates that the rotation implied by the 84-Ma polar shift would cause the maximum shift in paleoposition in the Atlantic and Indian oceans. The motions of Atlantic-bordering continents are well known since Cretaceous time, so we calculated the expected latitude shift for two sites in the Atlantic realm, one on North America (Washington, D.C.) and one on Africa (Dakar). First, we backtracked the inferred TPW rotation pole in Pacific coordinates (24.1°N, 195.8°E) into the hot spot reference frame (–6.1°N, 228.2°E) using the plate–hot spot motion model of Koppers (*7*). Washington and Dakar were backtracked into the hot spot reference frame using a model for motions of the Atlantic-bordering plates relative to the mantle (*44*). Finally, Washington and Dakar were rotated using the TPW motion pole in the hot spot reference frame. Because these two sites were located nearly 90° from the rotation pole, they moved nearly the full amount of rotation, mostly in paleolatitude.
39. W. Sager and U. Bleil, *Nature* **326**, 488 (1987).
40. R. A. Duncan and M. Storey, in *Synthesis of Results from Scientific Drilling in the Indian Ocean*, R. A. Duncan, D. K. Rea, R. B. Kidd, U. von Rad, J. K. Weissel, Eds. (American Geophysical Union, Washington, DC, 1992), pp. 91–103.
41. R. L. Parker, *J. Geophys. Res.* **93**, 3105 (1988).
42. A. A. P. Koppers, H. Staudigel, J. R. Wijbrans, M. S. Pringle, *Earth Planet. Sci. Lett.* **163**, 53 (1998).
43. M. S. Pringle, in *The Mesozoic Pacific: Geology, Tectonics, and Volcanism*, M. S. Pringle, W. W. Sager, W. V. Sliter, S. Stein, Eds. (American Geophysical Union, Washington, DC, 1993), pp. 187–215.
44. R. D. Müller, J.-Y. Royer, L. A. Lawver, *Geology* **21**, 275 (1993).
45. W. W. Sager, *J. Geophys. Res.* **89**, 6271 (1984).
46. ——— and B. H. Keating, *J. Geophys. Res.* **89**, 11135 (1984).
47. W. W. Sager, in *Geology and Offshore Mineral Resources of the Central Pacific Basin*, B. Keating and B. Bolton, Eds. (Springer-Verlag, New York, 1992), pp. 21–37.
48. C. G. A. Harrison. R. D. Jarrard, V. Vacquier, R. L. Larson, *Geophys. J. R. Astron. Soc.* **42**, 859 (1975).
49. J. A. Hildebrand and R. L. Parker, *J. Geophys. Res.* **92**, 12695 (1987).
50. W. W. Sager, R. A. Duncan, D. W. Handschumacher, in *The Mesozoic Pacific: Geology, Tectonics, and Volcanism*, M. S. Pringle, W. W. Sager, W. V. Sliter, S. Stein, Eds. (American Geophysical Union, Washington, DC, 1993), pp. 401–435.
51. W. W. Sager, thesis, University of Hawaii (1983).
52. P. Bryan, T. Shoberg, R. G. Gordon, K. E. Petronotis, D. D. Bergersen, in *The Mesozoic Pacific: Geology, Tectonics, and Volcanism*, M. S. Pringle, W. W. Sager, W. V. Sliter, S. Stein, Eds. (American Geophysical Union, Washington, DC, 1993), pp. 387–400.
53. Y. Ueda, *J. Geomagn. Geoelectr.* **49**, 1481 (1985).
54. J. Francheteau, C. G. A. Harrison, J. G. Sclater, M. L. Richards, *J. Geophys. Res.* **75**, 2035 (1970).
55. R. A. Duncan and D. A. Clague, *EOS Trans. Am. Geophys. Union* **65**, 1076 (1984).
56. S. O. Schlanger *et al.*, *J. Geophys. Res.* **89**, 11261 (1984).
57. K. Saito and M. Ozima, *Earth Planet. Sci. Lett.* **33**, 353 (1977).
58. M. S. Pringle and G. B. Dalrymple, in *The Mesozoic Pacific: Geology, Tectonics, and Volcanism*, M. S. Pringle, W. W. Sager, W. V. Sliter, S. Stein, Eds. (American Geophysical Union, Washington, DC, 1993), pp. 263–277.
59. E. L. Winterer *et al.*, in *The Mesozoic Pacific: Geology, Tectonics, and Volcanism*, M. S. Pringle, W. W. Sager, W. V. Sliter, S. Stein, Eds. (American Geophysical Union, Washington, DC, 1993), pp. 307–334.
60. M. S. Pringle and R. A. Duncan, *Proc. Ocean Drill. Program Sci. Results* **144**, 547 (1995).
61. Y. Takigami, I. Kaneoka, T. Ishii, Y. Nakamura, *Palaeogeogr. Palaeoclimatol. Palaeoecol.* **71**, 71 (1989).
62. We thank R. Gordon and an anonymous reviewer for constructive comments. Supported by NSF grants OCE98-11326 (W.W.S.) and OCE97-30394 (A.A.P.K.) and a TALENT-NATO grant by the Netherlands Science Foundation (NWO) (A.A.P.K.).

24 June 1999; accepted 18 November 1999